Warming sea surface temperatures fuel summer epidemics of eelgrass wasting disease

Maya L. Groner[1,2,*], Morgan E. Eisenlord[3], Reyn M. Yoshioka[4], Evan A. Fiorenza[5], Phoebe D. Dawkins[5], Olivia J. Graham[3], Miranda Winningham[3], Alex Vompe[6], Natalie D. Rivlin[7,8], Bo Yang[9], Colleen A. Burge[10,11], Brendan Rappazzo[12], Carla P. Gomes[12], C. Drew Harvell[3]

[1]US Geological Survey Western Fisheries Research Center, Seattle, WA 98115, USA
[2]Prince William Sound Science Center, Cordova, AK 99574, USA
[3]Department of Ecology and Evolutionary Biology, Cornell University, Ithaca, NY 14853, USA
[4]Oregon Institute of Marine Biology, University of Oregon, Charleston, OR 97420, USA
[5]Department of Ecology and Evolutionary Biology, University of California Irvine, Irvine, CA 92697, USA
[6]Department of Microbiology, Oregon State University, Corvallis, OR 97331, USA
[7]University of British Columbia, Vancouver, BC V6T 1Z1, Canada
[8]Institute of Marine Environmental Technology, University of Maryland Baltimore County, Baltimore, MD 21202, USA
[9]Department of Urban and Regional Planning, San José State University, San Jose, CA 95192, USA
[10]University of Maryland Baltimore, Department of Microbiology & Immunology, Baltimore, MD 21201, USA
[11]California Department of Fish & Wildlife, University of California, Davis Bodega Marine Laboratory, Bodega Bay, CA 94923, USA
[12]Department of Computer Science, Cornell University, Ithaca, NY 14853, USA

ABSTRACT: Seawater temperatures are increasing, with many unquantified impacts on marine diseases. While prolonged temperature stress can accelerate host–pathogen interactions, the outcomes in nature are poorly quantified. We monitored eelgrass wasting disease (EWD) from 2013–2017 and correlated mid-summer prevalence of EWD with remotely sensed seawater temperature metrics before, during, and after the 2015–2016 marine heatwave in the northeast Pacific, the longest marine heatwave in recent history. Eelgrass shoot density declined by 60% between 2013 and 2015 and did not recover. EWD prevalence ranged from 5–70% in 2013 and increased to 60–90% by 2017. EWD severity approximately doubled each year between 2015 and 2017. EWD prevalence was positively correlated with warmer temperature for the month prior to sampling while EWD severity was negatively correlated with warming prior to sampling. This complex result may be mediated by leaf growth; bigger leaves may be more likely to be diseased, but may also grow faster than lesions, resulting in lower severity. Regional stressors leading to population declines prior to or early in the heatwave may have exacerbated the effects of warming on eelgrass disease susceptibility and reduced the resilience of this critical species.

KEY WORDS: Labyrinthulomycetes · Seagrass · Opportunistic pathogens · Marine disease · Warm water anomaly · Heatwave · Heterokont

1. INTRODUCTION

Disease outbreaks can be particularly damaging when they affect ecosystem engineers such as corals, oysters, and seagrasses (Burge & Hershberger 2020). In seagrasses, wasting disease is one of myriad stressors associated with global population declines (Waycott et al. 2009, Martin et al. 2016, Sullivan et al. 2018). The largest known outbreak of wasting disease occurred in the 1930s along the European and North American coastlines of the Atlantic Ocean (Renn 1936). During this outbreak, eelgrass *Zostera*

marina meadows suffered up to 90% mortality. Impacts of the outbreak include altered sediment distribution, disrupted coastal food chains, and reductions in fisheries and migratory waterfowl (Short et al. 1988). In recent years, the dominant temperate seagrass of the Northern Hemisphere, eelgrass, has declined in some critical estuaries on both the US Atlantic and Pacific coasts (Lefcheck et al. 2017a, Harenčár et al. 2018), though stabilization and increases of some eelgrass populations have also been observed (Shelton et al. 2017, Lefcheck et al. 2017b). Causes of the degradation of these complex ecosystems are likely multi-factorial and are poorly understood. Although disease testing is rarely done, eelgrass wasting disease (EWD) outbreaks and elevated temperatures are hypothesized to be contributing to recent eelgrass declines in North America (Groner et al. 2014, Martin et al. 2016, Lefcheck et al. 2017a, Harenčár et al. 2018, Sullivan et al. 2018).

While marine disease outbreaks are frequently linked to short-term changes in temperature (Burge & Hershberger 2020), impacts of long-term warming on disease, particularly marine heatwaves, are less well explored (Harvell et al. 2019, Burge & Hershberger 2020). This is likely because few long-term data sets on disease prevalence in the oceans exist, and recognition of heatwaves as an important oceanographic phenomenon is recent, having only received a technical definition in 2016 (Hobday et al. 2016). Heatwaves, which occur when seawater temperatures exceed a threshold (usually the 90th percentile) of seasonally varying averaged temperatures for at least 5 consecutive days, are increasing in severity, duration, and intensity (Hobday et al. 2016, Oliver et al. 2018). The longest heatwave described to date occurred in the northeast Pacific Ocean from mid-2014 through 2016. Frequently called 'the blob', this heatwave was unprecedented in duration, intensity, and geographic scale. It was driven by both warm surface waters combined with unusually weak coastal winds that hindered upwelling events (Gentemann et al. 2017). Impacts of the heatwave included mass mortality of planktivorous seabirds, widespread harmful algal blooms, changes in plankton productivity and composition, and an outbreak of seastar wasting disease in numerous species, including the sunflower star *Pycnopodia helianthoides*, a keystone predator (Cavole et al. 2016, Gentemann et al. 2017, Harvell et al. 2019). These examples demonstrate that heatwaves can have dramatic and lasting ecosystem impacts, and underly the critical need to understand how these prolonged stressors alter host–pathogen interactions, particularly in ecosystem engineers.

EWD is caused by an opportunistic pathogen, *Labyrinthula zosterae* (*Lz*), that falls within the Labyrinthulomycetes (Muehlstein et al. 1991). *Lz* causes intracellular infections in leaf tissue, where it moves along a secreted mucus network to spread. Disease signs include black or brown lesions with defined borders and, often, a pale necrotic center (Muehlstein et al. 1991). *Lz* is sensitive to temperature, with faster *in vitro* growth documented at 18°C compared to 11°C for a strain isolated from the Salish Sea in WA, USA (Dawkins et al. 2018). Long-term studies (e.g. Bull et al. 2012) are needed to understand the full effect of temperature on EWD in the field and determine potential drivers of outbreaks. Recent studies have correlated heatwaves to substantial seagrass die-offs (Strydom et al. 2020), reduced restoration success (Aoki et al. 2020), and changes in fatty acid composition (Beca-Carretero et al. 2018), showing that seagrasses are sensitive to warming conditions. Little is known about how prolonged temperature shifts alter seasonal and multi-year patterns in EWD prevalence and severity or how these changes may influence the impact of EWD on populations (Bull et al. 2012, Groner et al. 2014, 2016, Dawkins et al. 2018, Sullivan et al. 2018, Brakel et al. 2019).

To investigate the extent of EWD and evaluate the hypotheses that EWD prevalence and severity are correlated with ocean warming, we surveyed eelgrass at 9 sites in the San Juan Islands, WA, spanning the years before, during, and after the 2015–2016 heatwave in the northeast Pacific. We quantified patterns of mid-summer EWD prevalence (% population diseased) and severity (% of an eelgrass blade with lesions) in the San Juan Islands from 2013–2017 and identified correlations between seasonal variation in remotely sensed seawater temperatures and field measurements of EWD prevalence, EWD severity, and eelgrass shoot density. To understand the association between *Lz* and EWD lesions, we quantified *Lz* infection loads in and adjacent to EWD lesions in field-collected plants.

2. MATERIALS AND METHODS

2.1. Survey design

Annual EWD surveys were conducted from 2013–2017 in late July through early August (days of the year 201–223) at 9 sites in the San Juan Islands, located within the Salish Sea in the Northeast Pacific (Fig. 1, Table 1). The sites were initially surveyed in 2013 (Groner et al. 2016). All sites were then re-
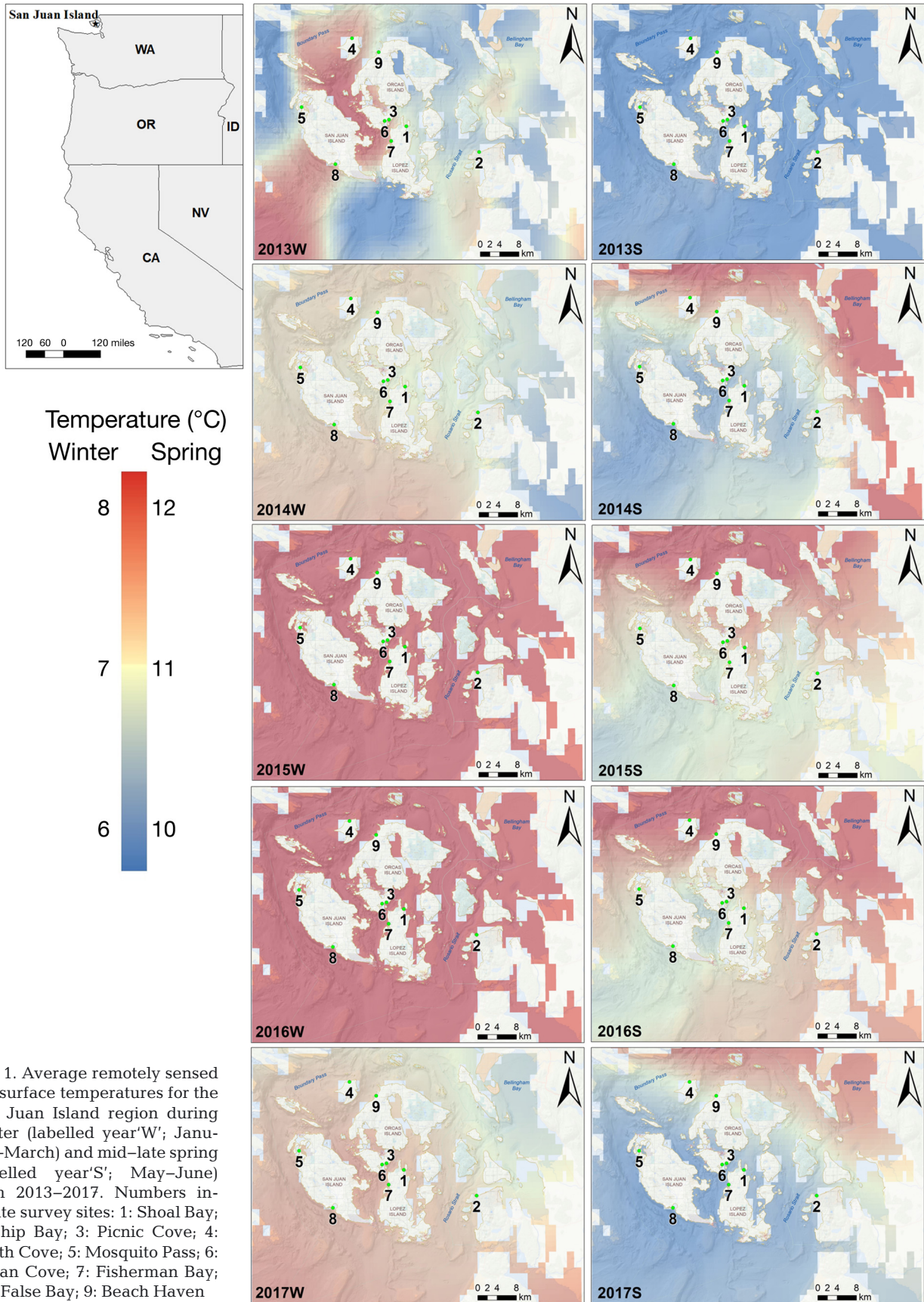
Fig. 1. Average remotely sensed sea surface temperatures for the San Juan Island region during winter (labelled year'W'; January–March) and mid–late spring (labelled year'S'; May–June) from 2013–2017. Numbers indicate survey sites: 1: Shoal Bay; 2: Ship Bay; 3: Picnic Cove; 4: North Cove; 5: Mosquito Pass; 6: Indian Cove; 7: Fisherman Bay; 8: False Bay; 9: Beach Haven

Table 1. Locations of eelgrass survey sites. Site ID corresponds with the locations in Fig. 1

ID	Site	Latitude (°N)	Longitude (°W)
1	Shoal Bay	48° 33.215′	122° 52.499′
2	Ship Harbor	48° 30.307′	122° 40.202′
3	Picnic Cove	48° 33.942′	122° 55.448′
4	North Cove	48° 42.287′	123° 03.221′
5	Mosquito Pass	48° 35.346′	123° 10.208′
6	Indian Cove	48° 33.773′	122° 56.078′
7	Fisherman Bay	48° 31.572′	122° 55.088′
8	False Bay	48° 28.975′	123° 04.451′
9	Beach Haven	48° 41.460′	122° 57.120′

surveyed in 2015 and 2017, and a subset was surveyed in 2014 and 2016. The timing of these surveys (mid-summer) captures the period when EWD prevalence and severity are approaching maximum levels (Short et al. 1988). Additional sampling was conducted at one site, Beach Haven, in 2016 to verify *Lz* as the etiologic agent of EWD lesions.

At each site, eelgrass samples were collected by hand at 2 m intervals along two 50 m transects laid parallel to the shore, 4 m apart, in the intertidal region. The midpoint between transects was placed ~1 m below mean lower low water (MLLW), with the shallowest transect between −1 and +1 MLLW and the deepest transect between −3 and −1 MLLW. Each 50 m transect was subdivided into five 10 m sections, and in each section the second oldest leaf was collected from 10 randomly selected shoots. The second oldest leaf was chosen for measurement of EWD because the disease is highly variable in medium-aged leaves such as this, providing a valuable metric for comparison within and across sites. Shoot density (number m^{-2}) was measured in 0.12 m^2 quadrats at 0, 25, and 50 m along the transect in 2013, and was not measured in 2014. In 2013, sampling occurred between 19 and 24 July. To minimize variation due to cumulative stress from summer low tides, all subsequent annual surveys (2014−2017) were conducted on the same tide series. The survey methods were slightly modified in 2015; transects were lengthened to 60 m and one shoot was sampled every 1 m along the transect. Shoot density was measured in 0.25 m^2 quadrats at 10, 30, and 50 m.

2.2. Measurements of EWD lesions

Collected leaves were taken to the University of Washington Friday Harbor Laboratories, WA, and kept at ambient seawater temperature until process-

ing (typically <24 h). Length and width of each leaf were measured, and leaves were diagnosed with EWD if they had lesions with irregular, dark, necrotic centers surrounded by a black border. Prevalence (presence/absence of EWD) was scored between 2013 and 2014, and severity (the proportion of the blade area with lesions) was also estimated from 2015−2017. Due to the constraints placed by the extensive training and laboratory hours needed to correctly identify and measure EWD lesions, a protocol was developed in 2016 to digitize images of sampled eelgrass blades and measure lesions digitally (Boese et al. 2008). All data collected in 2016 and 2017 were archived and analyzed digitally. Each leaf was cleaned, placed between 2 clear plastic sheets, and scanned at a resolution of 400−600 dpi using a Canon CanoScan 9000F Mark II scanner, creating a digital, high quality, permanent color image. The scanned image was used to diagnose and measure EWD lesions and measure leaf area. In 2016, measurements of leaf disease severity were made by a trained technician using ImageJ (Schneider et al. 2012). In 2017, measurements of lesion area and leaf area were aided by a machine-learning-powered web application. The web application assisted the technician by displaying the original scanned image overlaid with a disease prediction from a machine learning model. The human expert could then refine the prediction using the web application to obtain the lesion and leaf area metrics. To ensure that the change in methods did not alter the results, we compared severity measurements made using (1) the hand measurements vs. ImageJ (n = 60), and (2) the ImageJ measurements vs. the web app (n = 199) for a subset of samples, using a Bland-Altman test. For the first comparison, the ImageJ severity measurements were slightly larger (mean bias: 1.3%; 95% CI = −0.4 to 2.9%). For the second comparison, the ImageJ severity measurements were also slightly larger (0.9%; 0.3 to 1.4%).

2.3. Methods for acquiring remotely sensed sea surface temperature data

To relate EWD patterns to sea surface temperature (SST), remotely sensed SST data were acquired for our study area. SST values for all field sites were acquired for Dec 2012 to July 2017 (Fig. 1). Temperature values were extracted by geographical information system (GIS) tools via the Jet Propulsion Laboratory (JPL) OPeNDAP portal (JPL 2015). Group for High Resolution Sea Surface Temperature (GHRSST) Level 4 daily observations were acquired from the

NASA JPL. The GHRSST product masked out all land, and each pixel in the temperature imagery represents an SST value over a 1 × 1 km area. Three sites (North Cove, Indian Cove, False Bay) were identified at locations out of the ocean mask in the GHRSST product. For those sites, we extracted the nearest available ocean pixel within 2 km.

The procured remotely sensed SST data were a blended result from the Moderate Resolution Imaging Spectroradiometer (MODIS), Advanced Very High Resolution Radiometer (AVHRR), Advanced Along Track Scanning Radiometer (AATSR), Spinning Enhanced Visible and Infrared Imager (SEVIRI), Advanced Microwave Scanning Radiometer-EOS (AMSRE), Tropical Rainfall Measuring Mission Microwave Imager (TMI), Geostationary Operational Environmental Satellite (GOES) Imagery, and Multi-Functional Transport Satellite 1R (MTSAT-1R) radiometer (JPL 2010). A 2-dimensional variational data assimilation (2DVAR) method for blending the SST data from multiple observing platforms was used to generate the assimilated daily SST measurements (Chao et al. 2009). The spatial resolutions of AVHRR and MODIS SSTs are as high as 1 km. The frequent coverage and high spatial resolution of these infrared SSTs are sufficient for generating the blended SST fields on cloud-free days. Although thermal remote sensing cannot sense temperature with the presence of clouds or high concentrated aerosols (Wan 2014), longer wavelength microwave radiation can penetrate through cloud cover, haze, dust, and all but the heaviest rainfall. Consequently, microwave data from TMI (25 km) and AMSR-E (25 km) as well as *in situ* records from drifting and moored buoys were used to take part in the blending of the data set to produce continuous observations for the study region. A comparison of these fields using *in situ* observations specified that the blended SSTs via 2DVAR are accurate to less than 1°C in root-mean-square errors, comparable to the conventional SST observations (Chao et al. 2009).

2.4. Analysis of field data

Generalized linear mixed models and model selection, using Akaike's information criterion adjusted for small sample size (AICc) values, were used to quantify correlations between temperature metrics and multi-year trends in EWD prevalence, severity, and shoot density at all 9 sites using data from the 2013–2017 annual summer surveys and identify the best fitting model for each response variable (R v.4.0.3, packages 'lme4' [Bates et al. 2015] and 'AICcmodavg' [Mazerolle

2020]). Correlations between predictor variables and EWD presence or absence at the 9 survey sites were investigated using logistic regressions (n = 4829 eelgrass blades). Linear regression was used to quantify correlations between predictor variables and the severity of EWD in diseased blades between 2015 and 2017 (n = 2304). Linear regression was also used to quantify correlations between predictor variables and EWD density at all 9 sites using mean densities per transect from the shallowest and deepest transects from the 2013 and 2015–2017 surveys (n = 68). Predictor terms evaluated for all response variables via model selection included year, transect location within a site (low intertidal or high intertidal), leaf area, and a variety of temperature metrics (described below). In addition, EWD prevalence was included as a predictor variable for shoot density. Site was included as a random effect in all models.

Correlations between temperature, depth, year, and response variables were evaluated for each suite of models with the R package 'climwin' (Bailey & van de Pol 2016). We used this package to calculate and run models for all combinations of mean temperatures for time periods ranging from 1–6 mo in duration for the 6 mo prior to the date that the samples were collected. For each response variable (EWD presence, EWD severity, or shoot density), AICc was used to pick the best fitting model. Tests of so many combinations of temperature metrics can lead to overfitting of models and spurious correlations (Bailey & van de Pol 2016). To evaluate this possibility, we used the 'randwin' function to test the best model on 100 data sets with randomized climate data. Results from the best-fit model were compared to the distribution of results from the 100 randomized data sets to evaluate the probability that they fell within the 95% CI of the randomized results. Small p-values (i.e. p < 0.05) increase confidence that the effect of climate variables in the best fit model are not spurious. All best-fit models were examined for collinearity between predictor variables.

2.5. Methods for DNA extraction and quantitative PCR of *Lz* from eelgrass blades

A total of 28 eelgrass leaves with distinct EWD lesions of the type from which *Lz* can be readily cultured (i.e. dark black or brown in color without a white center) were collected from Beach Haven, WA, on 31 July 2016. To control for infection age, young leaves (1st or 2nd youngest within sheath) with solid, dark lesions and no other signs of degradation were

selected and processed within 24 h of collection using sterile techniques. After rinsing each leaf with reverse osmosis water, epiphytes were scraped from the surface of the leaf. To further clean the outer surface, the leaf was placed in sterile seawater and vortexed for 30 s on high. One ~2 cm^2 lesion was sampled from each leaf and extracted by cutting around the edge of the lesion. A similarly sized sample of green tissue with no lesions was selected from the same leaf ~3–5 cm distance from the lesion sample. The cut section was rinsed with reverse osmosis water, flash-frozen in liquid nitrogen, and stored at −80°C until DNA extraction. Frozen tissue (~60 mg) was ground to a fine powder using a Qiagen Tissue-Lyser II (25 Hz speed for 5 min).

Following published protocols (Groner et al. 2018a), DNA was extracted using the Qiagen DNeasy Mini Plant Kit. *Lz* cells were used for a standard curve (previously described in Groner et al. 2018a); the range of the cell curve was 1.37–13 720 cells reaction^{-1}. *Lz* DNA equivalents (*Lz* cells mg^{-1} of tissue) were quantified using quantitative PCR (qPCR) (Bockelmann et al. 2013, as modified by Groner et al. 2018a). The qPCR assay targeted the internal transcribed spacer (ITS) region (Bockelman et al. 2013) using the following forward (Laby_ITS_Taq_f: 5′-TTG AAC GTA ACA TTC GAC TTT CGT-3') and reverse (Laby_ITS_Taq_r: 5'-ACG CAT GAA GCG GTC TTC TT-3') primers and TaqMan probe (Laby_ITS_probe: FAM-5'-TGG ACG AGT GTG TTT TG-3'-MGB-NFQ). Each 20 µl reaction included 10 µl of TaqMan Fast Universal PCR Master Mix (Applied Biosystems by Life Technologies), 400 nm of each primer, 15 µg BSA, 100 nm probe, and 1–2 ng total DNA (1/10 dilution of extracted DNA). The cell curve was run in triplicate, and samples in duplicate in 96-well microplates using an Applied Biosystems 7500 Fast Real-Time PCR System with the following reaction conditions: 95°C for 20 s followed by 40 cycles of 95°C for 3 s and 60°C for 30 s. The reaction efficiency ranged from 101.2–102.9%, and R^2 > 0.99 for the standard curve. The detection limit was set at 1.37 cells. Amplification of 1.37 cells was achieved for all reactions in each cell curve.

2.6. Characterization of *Lz* loads in EWD lesions

The qPCR assay was used to detect and quantify *Lz* DNA abundance in paired lesioned and visually healthy leaf tissue from the same leaf (n = 28). Previous studies have confirmed the presence of *Lz* cells in lesioned eelgrass tissue with EWD through histology, pathogen culture, and inoculation, including the 2013 surveys used in this study (Groner et al. 2014, 2016, Dawkins et al. 2018). However, molecular testing to determine if infections were localized to the lesioned tissue or systemic throughout the leaf tissue was lacking for eelgrass collected in the San Juan Islands (Groner et al. 2018a).

3. RESULTS

3.1. Field surveys of mid-summer EWD prevalence and severity

EWD was present at all sites for all field sampling events; site-level disease prevalence (proportion of samples that were infected) ranged from 5–95% between 2013 and 2017; the highest levels for most sites occurred in 2017, when prevalence exceeded 60% at every site (Fig. 2a).

The best fitting model for the probability that a blade would be diseased included leaf area, transect depth (high intertidal or low intertidal), year, and the mean temperature for the month prior to sampling (conditional r^2 = 0.21, marginal r^2 = 0.17) (Table 2, Fig. 3). Disease risk among sites was positively correlated with leaf area, temperature, and was higher in the high intertidal transects compared to the low intertidal transects. The risk of EWD was similar from 2013–2016 but increased substantially in 2017 (Fig. 3). There were no other models with ΔAICc < 3 relative to the best fitting model (Fig. 4a). Comparison of the best-fit 'climwin' model against results of 100 data sets with randomized temperature data showed that the temperature effect was unlikely to be due to model overfitting (p < 0.0001).

Between 2015 and 2017, the average severity of visibly diseased plants approximately doubled each year, from 0.8% (percent of the blade with visible lesions) in 2015 to 1.6% in 2016 to 3.4% in 2017 (Fig. 2b). The best fitting model included terms for year, leaf area, and the mean temperature for 1 mo beginning 3 mo prior to sampling (conditional r^2 = 0.14, marginal r^2 = 0.07) (Table 2, Fig. 5). EWD severity was negatively correlated with leaf area and temperature. After controlling for the effects of leaf area and temperature, disease severity was slightly lower in 2016 and much higher in 2017 compared to 2015. This difference is illustrated in Fig. 3, which depicts the predicted disease severity for Beach Haven. Numerous additional models had a ΔAICc < 3 relative to the best fitting model (Fig. 4b). These models
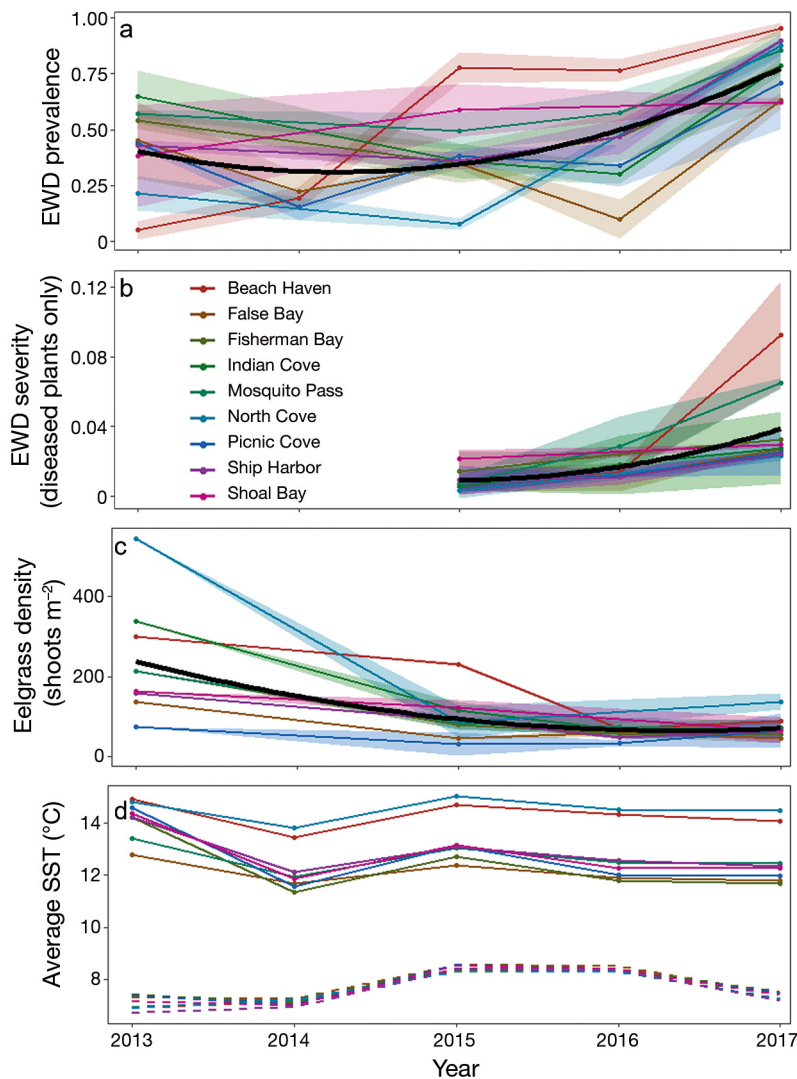
Fig. 2. Patterns of (a) eelgrass wasting disease (EWD) prevalence (% infected), (b) EWD severity, (c) eelgrass shoot density, and (d) sea surface temperature (SST) in the San Juan Islands from 2013–2017; EWD severity was calculated only for 2015–2017. In (d), Group for High Resolution Sea Surface Temperature (GHRSST) averaged temperatures were used to calculate means; dashed lines: mean SSTs averaged across January, February, and March; solid lines: average across July. In (a–c), black lines: averaged responses; shaded areas: SE

Eelgrass shoot density was most affected by the year and site of the survey. Relative to 2013, all other survey years had lower density. Intertidal eelgrass shoot density declined by nearly 60% between 2013 and 2015 (from 237 ± 139 to 98 ± 57 shoots m^{-2}) and remained at similarly low levels through 2017 (Fig. 2c). The best model for shoot density included the term year (conditional r^2 = 0.68, marginal r^2 = 0.47) (Table 2). While AICc values from one 'climwin' model indicated that a term for the average temperature for the 2 mo period that began 7 mo prior to sampling improved model fit relative to a model without this temperature term (ΔAICc = 7.6), this result was likely spurious. Comparison of this model against 100 'climwin' models with randomized climate data indicated that the detected temperature effect was spurious, as effect size for the temperature effect in the best-fit model was not statistically different from a model with randomized temperature data (p = 0.95). Therefore, we conservatively presented the model without a temperature term.

For all of the above models, winter temperatures (beginning 7–4 mo prior to sampling) were strongly collinear with the fixed effects of study year; therefore, confounding of these variables prevented determination of how winter temperatures may have been correlated with response variables (EWD presence, EWD severity, or eelgrass density).

incorporated temperature windows that did and did not overlap with the best fitting model. This suggests that while temperature is important in predicting disease severity, the data set used in this analysis could not identify the most predictive temperature window. No other temperature windows were collinear with predictor variables. Comparison of the best-fit model against analytical results of 100 data sets with randomized temperature data showed that the temperature effect was unlikely to be due to model overfitting (p = 0.0003).

3.2. Characterization of *Lz* loads in EWD lesions from field-collected samples

All 28 field-collected eelgrass sections with visually identified EWD lesions had high concentrations of *Lz* while the corresponding leaf sections taken from visually healthy tissue on the same leaf were negative for *Lz* (Fig. 5). Lesioned tissue samples had *Lz* DNA equivalent to 434 ± 132 (mean ± SE) cells mg^{-1} wet tissue, while *Lz* DNA in the paired green tissue was below the qPCR detection limit.

Table 2. Best fitting models for disease status, disease severity and eelgrass shoot density in mid-summer in the San Juan Islands. Model results for the (a) probability that an eelgrass leaf would be diseased during 2013–2017; (b) severity of eelgrass wasting disease (EWD) from 2015 through 2017. (c) Results of best fitting model for eelgrass shoot density during 2013–2017 (excluding 2014). For all models, the earliest year of data and the site of Beach Haven served as the reference case. In the first model, the reference case was the lower intertidal transect. Model selection was performed to minimize Akaike's information criterion for small sample size (AICc) scores. **Bold** font indicates significance (p ≤ 0.05)

(a) EWD presence	Estimate	SE	z	p
Intercept	**−13.82**	**2.63**	**−5.3**	**<0.0001**
Temperature (for month prior to sampling)	**0.48**	**0.08**	**5.6**	**<0.0001**
Temperature (January and February)	**0.89**	**0.39**	**2.3**	**0.02**
Leaf area (dm^2)	**0.1**	**0.01**	**6.9**	**<0.0001**
Shallow	**0.17**	**0.07**	**2.5**	**0.01**
Year 2014	**−1.23**	**0.24**	**−5**	**<0.0001**
Year 2015	−1.1	0.59	−1.9	0.06
Year 2016	−0.54	0.51	−1.1	0.29
Year 2017	**2.3**	**0.23**	**9.9**	**<0.0001**
(b) EWD severity	Estimate	SE	df	t p
Intercept	**0.219**	**0.034**	**971**	**6.4 <0.0001**
Temperature (for 1 mo, 3 mo prior to sampling)	**−0.014**	**0.003**	**2011**	**−4.7 <0.0001**
Year 2016	**−0.018**	**0.006**	**2299**	**−3.2 0.001**
Year 2017	**0.013**	**0.006**	**2216**	**2.2 0.028**
Leaf area (dm^2)	**−0.004**	**0.001**	**2289**	**−4.9 <0.0001**
(c) Eelgrass shoot density				
Intercept	**237.3**	**22.6**	**15.2**	**10.5 <0.0001**
Year 2015	**−138.2**	**20.2**	**55.7**	**−6.8 <0.0001**
Year 2016	**−166.6**	**22.0**	**56.5**	**−7.6 <0.0001**
Year 2017	**−163.4**	**20.2**	**55.7**	**−8.1 <0.0001**

4. DISCUSSION

Our results document a region-wide reduction in eelgrass shoot density in the San Juan Islands, followed by an increase in EWD prevalence and severity. The timing of the increasing disease outbreak (during and after the 2015–2016 heatwave) contributes to a growing body of literature suggesting that marine heatwaves may intensify host–pathogen interactions and drive declines in ecosystem engineers (Caldwell et al. 2016, Harvell et al. 2019). This timing of the heatwave may have exacerbated already stressed eelgrass meadows, as indicated by the shoot density declines that occurred before the heatwave. 2015 and 2016 were the warmest years on record in the San Juan Islands (Gentemann et al. 2017), and both winter and spring temperatures were 1–1.5°C warmer than the other 3 survey years (Figs. 1 & 2). These conditions coincided with an outbreak of EWD. At the beginning of the heatwave, shoot density had declined by 60% in intertidal meadows relative to 2013 values and remained low throughout the rest of the study. EWD prevalence increased at some sites in 2016 and at all sites in 2017. By 2017, the mid-summer prevalence was above 60% at all sites. The severity of
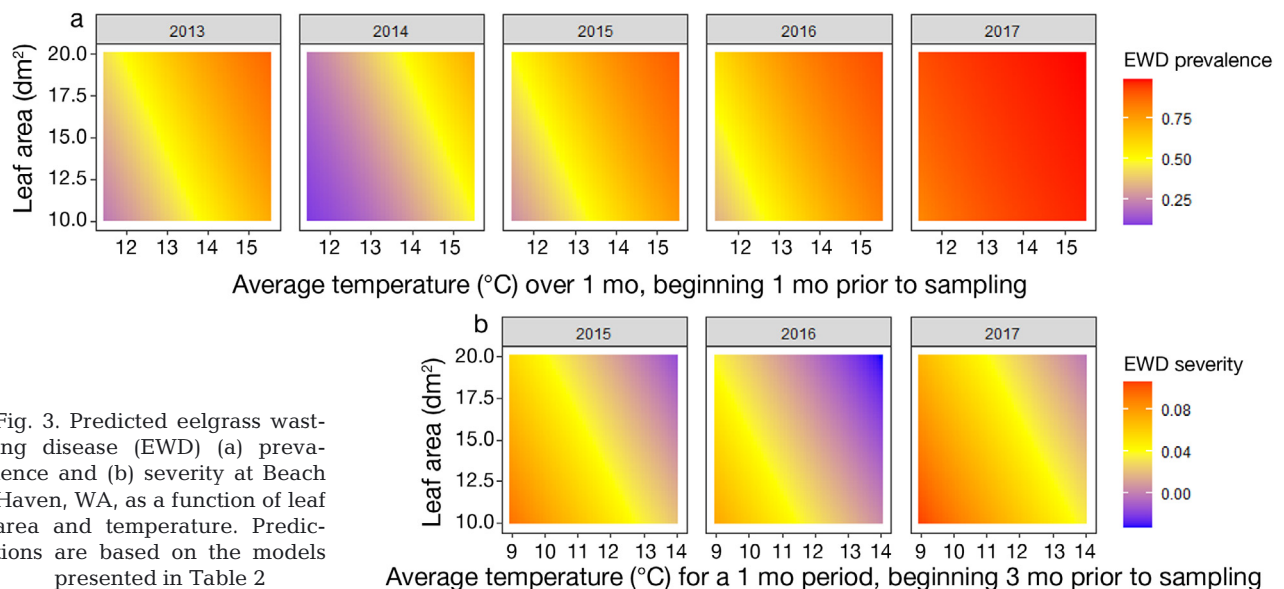

Fig. 3. Predicted eelgrass wasting disease (EWD) (a) prevalence and (b) severity at Beach Haven, WA, as a function of leaf area and temperature. Predictions are based on the models presented in Table 2
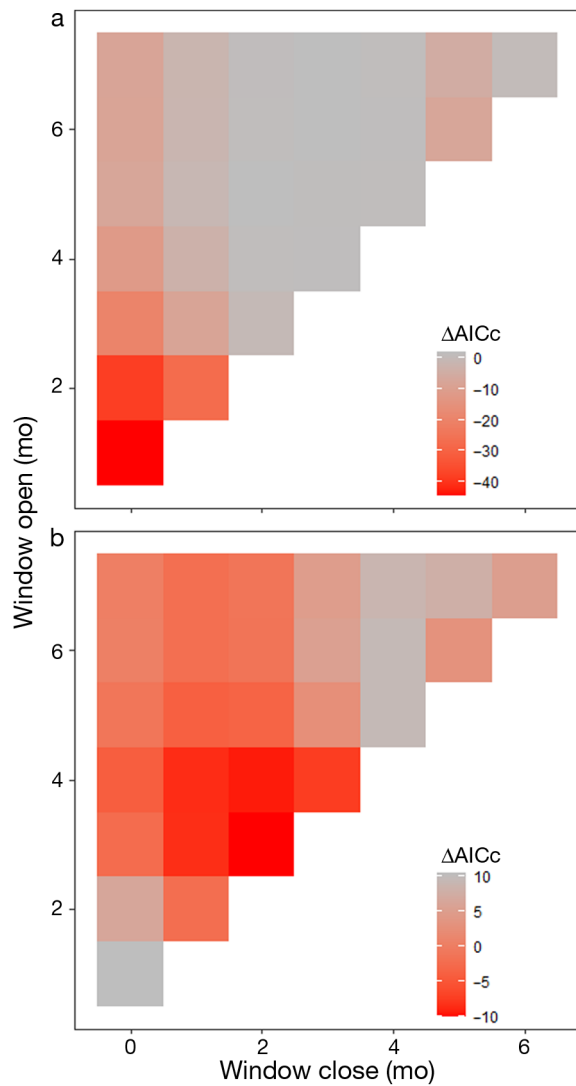
Fig. 4. Difference in Akaike's information criterion adjusted for small sample size (ΔAICc) values between 'climwin' models of (a) eelgrass wasting disease (EWD) presence and (b) EWD severity. For each scenario, all models included the predictors described in Table 2, but the temperature metrics were varied to include mean temperatures across a variety of time windows (from 1–7 mo long) beginning 7 mo prior to sampling events (*y*-axis) and ending 0 mo prior to sampling events (*x*-axis). The ΔAICc value is the difference between the model with and without the temperature predictor. Note that the values of the color keys differ between panels

Fig. 5. (a) *Labyrinthula zosterae* (*Lz*) DNA detected using quantitative PCR in lesioned and visually healthy eelgrass tissue sampled from the same plant (n = 28); error bars: ±1 SE. (b) Eelgrass segments showing lesioned (left) and healthy tissue (right)

EWD infections doubled each year between 2015 and 2017, accompanying the steep rise in prevalence. While a longer time-series would be valuable for better understanding pre- and post-outbreak conditions, the data collected document increasing EWD prevalence and severity coinciding with and extending beyond the 2015–2016 heatwave.
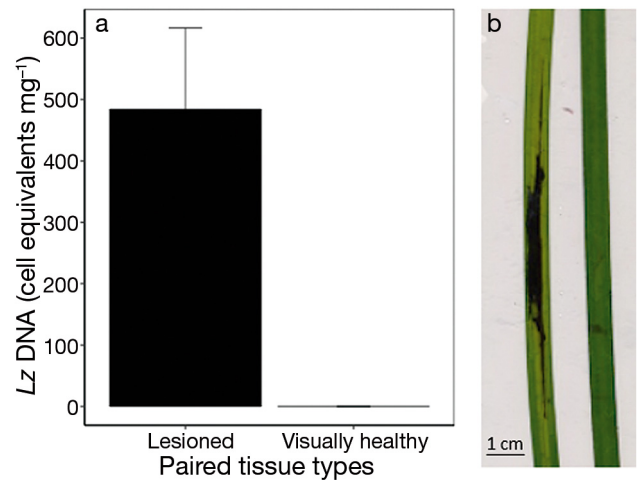
Mid-summer EWD prevalence was positively correlated with early summer temperatures (i.e. averaged across the month prior to sampling), while mid-summer EWD severity was negatively correlated with spring warming (i.e. monthly averaged temperature 3 mo prior to sampling). A link between EWD and temperature has been identified in past studies (e.g. Bull et al. 2012, Dawkins et al. 2018, Brakel et al. 2019). For example, *Labyrinthula* sp. has been found to grow faster at warmer temperatures (18°C compared to 11°C) in culture (Dawkins et al. 2018). In a 14 yr field study (1997–2010), increased EWD prevalence and EWD-driven declines in August in the Isles of Scilly were associated with warmer temperatures in July (Bull et al. 2012). Laboratory studies have also shown that the effects of temperature on EWD are dependent upon other conditions. For example, under laboratory conditions, high temperatures (27°C compared to 22°C) in combination with low light increases EWD and plant mortality (Brakel et al. 2019). The higher prevalence of disease found at shallow depths may have been driven by localized variations in temperature that would not have been accounted for in the remotely sensed temperature data used in the analysis. During summer low tides, shallower transects are exposed to air temperatures for longer periods. Increased disease prevalence of plants in shallower intertidal transects has been observed in previous studies in this region (e.g. Groner et al. 2014).

The correlation between warmer temperature and decreased EWD severity is likely due to temperature

causing eelgrass growth to outpace *Lz* growth. Disease severity is calculated as a proportion of blade area. Larger eelgrass blades have consistently lower disease severity than smaller blades, likely because the rapid expansion rate of the larger blades exceeds the rate the EWD lesions spread. During warm springs, blade growth is likely further accelerated and may outpace lesion growth so that EWD severity is negatively correlated with warmer spring temperatures. The inverse effects of temperature on disease transmission and progression suggest that both EWD metrics as well as eelgrass growth rates are required to assess the health of eelgrass beds. In years with conditions promoting accelerated plant growth, eelgrass may experience more disease, but may also experience fewer impacts of disease as a result of greater photosynthetic capacity. In contrast, both severity and disease prevalence were higher in 2017, suggesting that some conditions can promote both disease transmission and progression. The disease severity documented in this study represents a single timepoint across a changing trajectory. Disease severity typically increases throughout the summer and would be expected to peak 1–2 mo after the surveys in this study were completed. Mortality of eelgrass is typically associated with higher levels of disease severity than were observed in this field study (e.g. Groner et al. 2018a). The sublethal impacts of EWD are not well studied.

Due to the limited among-site variation in winter temperature within years and high multicollinearity between winter temperature and 'year' effects, this study had little statistical power for detecting effects of winter temperature on disease prevalence or severity. Winter warming is a common risk factor for other infectious marine diseases with pronounced seasonal cycles, including epizootic shell disease in American lobsters (Groner et al. 2018b) and several coral diseases (Caldwell et al. 2016), although the impact of winter heatwaves on subsequent summer disease is not well explored. Little is currently known about the low temperature tolerance of *Lz* or any aspects of its over-wintering biology. Further work to investigate the impacts of winter warming on EWD will be valuable to identify the role of winter temperature variability.

While we assessed the correlations between temperature metrics and EWD metrics, numerous other environmental and ecological changes in the Salish Sea accompanied the 2015–2016 heatwave, including increases in harmful algal blooms, altered food webs with increases in warm water species and lower overall biomass, and shifted phenology of key

ecological events (such as plankton blooms, which can impact light availability to eelgrass) (Cavole et al. 2016). Although temperature has been previously shown to increase the risk of EWD and is correlated with EWD prevalence in this study, it is realistic to also investigate other synergistic factors as contributors to infection risk.

Eelgrass is a highly plastic plant, and changes in morphology and shoot density can reflect both adaptive plasticity to changing environmental conditions or declines in condition (Backman 1991, Bertelli et al. 2021). However, the continued lack of recovery in shoot density after a 60% decline detected at the beginning of the heatwave in 2015 signals a potential threat to the continued viability of the intertidal portion of these eelgrass meadows and suggests that other factors may have been reducing eelgrass populations prior to the heatwave. We did not identify an effect of temperature on shoot density, possibly due to the relatively low sample size for this response variable. Nonetheless, the high levels of disease and strong negative effect of the years during and after the heatwave (2015–2017) on eelgrass density suggest that conditions during the heatwave reduced eelgrass resilience following an initial decline. Abrupt and persistent changes in the community structure of numerous marine ecosystems have been documented in response to the occurrence of this same heatwave in the Gulf of Alaska, suggesting that many ecosystems have reached alternative equilibria or are recovering slowly (Suryan et al. 2021). In a study of eelgrass resilience across ~225 km of eelgrass meadows in Atlantic Canada, sites with high mean temperatures, in shallower locations with fewer currents, and with high levels of short-term temperature variation experienced the greatest reductions in resilience (Krumhansl et al. 2021). This was hypothesized to occur because the plant carbon demand increases with temperature. When carbon is not available externally it may be provided from the rhizome, resulting in an overall reduction in below-ground carbohydrate storage and potentially reducing capacity to respond to future stressors (Fraser et al. 2014). It is unknown if continued exposure to disease may cause similar reductions to below-ground biomass. Many of the sites described in our study meet the environmental criteria associated with reduced resilience to stressors in Atlantic Canada. Continued monitoring of a subset of these eelgrass sites has continued and will be valuable for quantifying meadow recovery and potential density-dependent feedbacks on transmission.

Our molecular work verified that *Lz* is concentrated within the distinctive black lesions character-

istic of EWD. High concentrations of *Lz* DNA within lesions and the lack of detectable *Lz* DNA in adjacent healthy green tissue confirm that the pathogen is localized. This finding is consistent with earlier histological analyses (Groner et al. 2014) and confirms the presence of *Lz* in these lesions.

This study highlights the importance of evaluating the impact of long-term exposures to warming on host–pathogen interactions. The correlations between SSTs and EWD prevalence and severity suggest that conditions prior to and associated with the 2015–2016 marine heatwave played a role in the intensifying outbreak. However, this conclusion does not exclude the possibility that the drivers of this outbreak were multifactorial and may have also included factors aside from temperature such as turbidity and/or changes to the leaf microbiome (Sullivan et al. 2018). Future research on understanding the mechanism(s) driving the correlations between temperature and disease, measuring the population-level impacts of EWD, and identifying factors that influence the resilience of this critical ecosystem engineer to disease will improve our understanding of this complex disease.

LITERATURE CITED

Aoki LR, McGlathery KJ, Wiberg PL, Al-Haj A (2020) Depth affects seagrass restoration success and resilience to marine heat wave disturbance. Estuaries Coasts 43: 316–328

Backman TWH (1991) Genotypic and phenotypic variability of *Zostera marina* on the west coast of North America. Can J Bot 69:1361–1371

Bailey LD, van de Pol M (2016) climwin: an R toolbox for climate window analysis. PLOS ONE 11:e0167980

Bates D, Mächler M, Bolker B, Walker S (2015) Fitting linear mixed-effects models using lme4. J Stat Softw 67:1–48

Beca-Carretero P, Guihéneuf F, Marín-Guirao L, Bernardeau-Esteller J, García-Muñoz R, Stengel DB, Ruiz JM (2018) Effects of an experimental heat wave on fatty acid composition in two Mediterranean seagrass species. Mar Pollut Bull 134:27–37

Bertelli CM, Bull JC, Cullen-Unsworth LC, Unsworth RKF (2021) Unravelling the spatial and temporal plasticity of eelgrass meadows. Front Plant Sci 12:664523

Bockelmann AC, Tams V, Ploog J, Schubert PR, Reusch TB (2013) Quantitative PCR reveals strong spatial and temporal variation of the wasting disease pathogen, *Labyrinthula zosterae* in northern European eelgrass (*Zostera marina*) beds. PLOS ONE 8:e62129

Boese BL, Clinton PJ, Dennis D, Golden RC, Kim B (2008) Digital image analysis of *Zostera marina* leaf injury. Aquat Bot 88:87–90

Brakel J, Jakobsson-Thor S, Bockelmann AC, Reusch TBH (2019) Modulation of the eelgrass–*Labyrinthula zosterae* interaction under predicted ocean warming, salinity change and light limitation. Front Mar Sci 6:268

Bull JC, Kenyon EJ, Cook KJ (2012) Wasting disease regulates long-term population dynamics in a threatened seagrass. Oecologia 169:135–142

Burge CA, Hershberger PK (2020) Climate change can drive marine diseases. In: Behringer DC, Silliman BR, Lafferty KD (eds) Marine disease ecology. Oxford University Press, New York, NY p 83–94

Caldwell JM, Heron SF, Eakin EM, Donahue MJ (2016) Satellite SST-based coral disease outbreak predictions for the Hawaiian Archipelago. Remote Sens (Basel) 8:93

Cavole LM, Demko AM, Diner RE, Giddings A and others (2016) Biological impacts of the 2013–2015 warm-water anomaly in the Northeast Pacific: winners, losers, and the future. Oceanography (Wash DC) 2:273–285

Chao Y, Li Z, Farrara JD, Hung P (2009) Blending sea surface temperatures from multiple satellites and in situ observations for coastal oceans. J Atmos Ocean Technol 26:1415–1426

Dawkins PD, Eisenlord ME, Yoshioka RM, Fiorenza E and others (2018) Environment, dosage, and pathogen isolate moderate virulence in eelgrass wasting disease. Dis Aquat Org 130:51–63

Fraser MW, Kendrick GA, Statton J, Hovey RK, Zavala-Perez A, Walker DI (2014) Extreme climate events lower resilience of foundation seagrass at edge of biogeographical range. J Ecol 102:1528–1536

Gentemann CL, Fewings MR, García-Reyes M (2017) Satellite sea surface temperatures along the west coast of the United States during the 2014–2016 northeast Pacific marine heat wave. Geophys Res Lett 44:312–319

Groner ML, Burge CA, Couch CS, Kim CJ and others (2014) Host demography influences the prevalence and severity of eelgrass wasting disease. Dis Aquat Org 108:165–175

Groner ML, Burge CA, Kim CJS, Rees EE and others (2016) Plant characteristics associated with widespread variation in eelgrass wasting disease. Dis Aquat Org 118:159–168

Groner ML, Burge CA, Cox R, Rivlin ND and others (2018a) Oysters and eelgrass: potential partners in a high pCO₂ ocean. Ecology 99:1802–1814

Groner ML, Shields JD, Landers DF Jr, Swenarton J, Hoenig JM (2018b) Rising temperatures, molting phenology, and epizootic shell disease in the American lobster. Am Nat 192:E163–E177

Harenčár JG, Lutgen GA, Taylor ZM, Saarman NP, Yost JM (2018) How population decline can impact genetic diversity: a case study of eelgrass (*Zostera marina*) in Morro Bay, California. Estuaries Coasts 41:2356–2367

Harvell CD, Montecino-Latorre D, Caldwell JM, Burt JM and others (2019) Disease epidemic and a marine heat wave are associated with the continental-scale collapse of a pivotal predator (*Pycnopodia helianthoides*). Sci Adv 5:eaau7042

Hobday AJ, Alexander LV, Perkins SE, Smale DA and others (2016) A hierarchical approach to defining marine heatwaves. Prog Oceanogr 141:227–238

JPL (2010) OurOcean Project. GHRSST Level 4 G1SST Global Foundation Sea Surface Temperature Analysis. Ver. 1. PO.DAAC, Pasadena, CA. https://doi.org/10.5067/GHG1S-4FP01 (accessed 28 Febraury 2020)

JPL (2015) MUR MEaSUREs Project. GHRSST Level 4 MUR Global Foundation Sea Surface Temperature Analysis. Ver. 4.1. PO.DAAC, Pasadena, CA. https://doi.org/10.5067/GHGMR-4FJ04 (accessed 10 February 2020)

Krumhansl KA, Dowd M, Wong MC (2021) Multiple metrics of temperature, light, and water motion drive gradients in eelgrass productivity and resilience. Front Mar Sci 8:48

Lefcheck JS, Wilcox DJ, Murphy RR, Marion SR, Orth RJ (2017a) Multiple stressors threaten the imperiled coastal foundation species eelgrass (*Zostera marina*) in Chesapeake Bay, USA. Glob Change Biol 23:3474–3483

Lefcheck JS, Marion SR, Orth RJ (2017b) Restored eelgrass (*Zostera marina* L.) as a refuge for epifaunal biodiversity in mid-western Atlantic coastal bays. Estuaries Coasts 40:200–212

Martin DL, Chiari Y, Boone E, Sherman TD and others (2016) Functional, phylogenetic and host-geographic signatures of *Labyrinthula* spp. provide for putative species delimitation and a global-scale view of seagrass wasting disease. Estuaries Coasts 39:1403–1421

Mazerolle MJ (2020) AICcmodavg: Model selection and multimodel inference based on (Q)AIC(c). https://cran.r-project.org/package=AICcmodavg

Muehlstein LK, Porter D, Short FT (1991) *Labyrinthula zosterae* sp. nov., the causative agent of wasting disease of eelgrass, *Zostera marina*. Mycologia 83:180–191

Oliver ECJ, Donat MG, Burrows MT, Moore PJ and others (2018) Longer and more frequent marine heatwaves over the past century. Nat Commun 9:1324

Renn CE (1936) The wasting disease of *Zostera marina*. I. A phytological investigation of the diseased plant. Biol Bull (Woods Hole) 70:148–158

Schneider CA, Rasband WS, Eliceiri KW (2012) NIH Image to ImageJ: 25 years of image analysis. Nat Methods 9:671–675

Shelton AO, Francis TB, Feist BE, Williams GD, Lindquist A, Levin PS (2017) Forty years of seagrass population stability and resilience in an urbanizing estuary. J Ecol 105:458–470

Short FT, Ibelings BW, Den Hartog C (1988) Comparison of a current eelgrass disease to the wasting disease in the 1930s. Aquat Bot 30:295–304

Strydom S, Murray K, Wilson S, Huntley B and others (2020) Too hot to handle: unprecedented seagrass death driven by marine heatwave in a World Heritage Area. Glob Change Biol 26:3525–3538

Sullivan BK, Trevathan-Tackett SM, Neuhauser S, Govers LL (2018) Host–pathogen dynamics of seagrass diseases under future global change. Mar Pollut Bull 134:75–88

Suryan RM, Arimitsu ML, Coletti HA, Hopcroft RR and others (2021) Ecosystem response persists after a prolonged marine heatwave. Sci Rep 11:6235

Wan Z (2014) New refinements and validation of the collection-6 MODIS land-surface temperature/emissivity product. Remote Sens Environ 140:36–45

Waycott M, Duarte CM, Carruthers TJB, Orth RJ and others (2009) Accelerating loss of seagrasses across the globe threatens coastal ecosystems. Proc Natl Acad Sci USA 106:12377–12381